DOI: 10.1002/ejic.200600631

Synthesis and Structure of $[n\mathrm{Pr_3N(CH_2)_6N}n\mathrm{Pr_3}][\mathrm{CuFe_3Br_3(SePh)_6}]$, $[\mathrm{Cu_5Fe(SePh)_7(PPh_3)_4}]$ and $[\mathrm{Cu_4Fe_3(SePh)_{10}(PPh_3)_4}]$

Andreas Eichhöfer,*[a] Dieter Fenske,[a,b] and Jolanta Olkowska-Oetzel[a]

Dedicated to Michael Binnewies on the occasion of his 60th birthday

Keywords: Iron / Copper / Selenium / Cluster compounds

CuBr and $Fe(OOCCH_3)_2$ react with $PhSeSiMe_3$ in acetonitrile in the presence of the diammonium salt $[n\mathrm{Pr_3N(CH_2)_6N}n\mathrm{Pr_3}]\mathrm{Br_2}$ to yield ionic $[n\mathrm{Pr_3N(CH_2)_6N}n\mathrm{Pr_3}][\mathrm{CuFe_3Br_3(SePh)_6}]$. The neutral complexes $[\mathrm{Cu_5Fe(SePh)_7(PPh_3)_4}]$ and $[\mathrm{Cu_4Fe_3(SePh)_{10}(PPh_3)_4}]$ were obtained by similar reactions of different stoichiometric mixtures of $CuOOCCH_3$ and $FeCl_2$ with PPh_3 and $PhSeSiMe_3$. The crystal structures of the compounds were determined by single-crystal X-ray analysis to give new structural types of molecular cluster compounds formed by copper, iron and selenium. Thermal treatment of $[\mathrm{Cu_5Fe(SePh)_7(PPh_3)_4}]$ and $[\mathrm{Cu_4Fe_3(SePh)_{10}(PPh_3)_4}]$ results in the formation of mixtures of binary Cu_2Se and ternary $CuFeSe_2$.

Introduction

The synthesis of ternary cluster molecules has attracted interest recently. Examples of different compounds include $(PPh_4)[Cu_6In_3(SEt)_{16}]$,[1] $[M^I{}_6M^{III}{}_8Cl_4E_{13}(PPh_3)_6]$ (M^I = Cu, Ag; M^{III} = Ga, In; E = S, Se),[2] $[Cu_{11}In_{15}Se_{16}(SePh)_{24}(PPh_3)_4]$,[3] $[Ag_{26}In_{18}S_{36}Cl_6(dppm)_{10}(thf)_4][InCl_4(thf)]_2$,[4] $[Hg_{15}Cu_{20}S_{25}(Pn\mathrm{Pr_3})_{18}]$,[5,6] $[Cu_4Nb_2Se_6(PMe_3)_8]$,[7] $[Ta_4Cu_{12}Cl_8S_{12}(PMe_3)_{12}]$,[8] $[(N,N'\text{-tmeda})_5Zn_5Cd_{11}Se_{13}(SePh)_6(thf)_2]$,[9] and $[(py)_8Ln_4M_2Se_6(SePh)_4]$ (Ln = Er, Yb, Lu; M = Cd, Hg).[10] Interest in these compounds lies in the characterization of their structures and an investigation of their properties. In this context, Kanatzidis et al. have studied the suitability of mixed copper/indium chalcogenolates as precursor materials for the photovoltaic materials $CuInE_2$ (E = S, Se).[1,11] Corrigan et al. have observed room-temperature fluorescence for the ternary 12-12′-16 cluster (12 = Zn; 12′ = Cd; 16 = Se) $[(N,N'\text{-tmeda})_5Zn_5Cd_{11}Se_{13}(SePh)_6(thf)_2]$,[9] while binary cadmium or zinc selenide clusters show weak luminescence only at temperatures below 50 K.[12,13] Strong infrared fluorescence behavior has been observed to occur in the heterometallic chalcogenido cluster molecules $[(py)_8Ln_4M_2Se_6(SePh)_4]$ (Ln = Er; M = Cd, Hg).[10]

The ternary phase $CuFeS_2$ has been known to be a semiconductor material for a long time and was one of the first compounds to be used for the construction of radio frequency detectors,[14] while information about $CuFeSe_2$ is limited and only a few papers have been devoted to this compound during the last five years.[15] Until now only a limited number of cluster compounds have been synthesized that contain copper, iron and sulfur or selenium; these include $[Fe_3Cu(Si\mathrm{Pr})_6Cl_3]^{2-}$,[16] $[Fe_3Cu(Se\mathrm{Pr})_6Cl_3]^{2-}$, and $[Fe_2Cu_4(Si\mathrm{Pr})_8Cl_3]^{2-}$.[17] Here we report the synthesis and characterization of three new compounds of this type, namely $[n\mathrm{Pr_3N(CH_2)_6N}n\mathrm{Pr_3}][\mathrm{CuFe_3Br_3(SePh)_6}]$, $[\mathrm{Cu_5Fe(SePh)_7(PPh_3)_4}]$ and $[\mathrm{Cu_4Fe_3(SePh)_{10}(PPh_3)_4}]$.

Results and Discussion

Synthesis

Reaction of a 1:3 mixture of CuBr and $Fe(OOCCH_3)_2$ with $PhSeSiMe_3$ in acetonitrile in the presence of the diammonium salt $[n\mathrm{Pr_3N(CH_2)_6N}n\mathrm{Pr_3}]\mathrm{Br_2}$ yielded, after layering with diethyl ether, dark red-orange crystals of **1** after a few days (Scheme 1).

The use of the neutral ligand PPh_3 instead of the diammonium salt $[n\mathrm{Pr_3N(CH_2)_6N}n\mathrm{Pr_3}]\mathrm{Br_2}$ in reactions of $CuOOCCH_3$ and $FeCl_2$ with $PhSeSiMe_3$ led to the formation of dark-red solutions from which red crystals of **2** (Scheme 2) grew over the course of several days.

A similar reaction with a 1:0.8 ratio of $CuOOCCH_3$ and $FeCl_2$ yielded red-orange crystals of **3** (Scheme 3).

[a] Institut für Nanotechnologie, Forschungszentrum Karlsruhe, Postfach 3640, 76021 Karlsruhe, Germany
Fax: +49-7247-82-6368
E-mail: eichhoefer@int.fzk.de
[b] Institut für Anorganische Chemie der Universität, Engesserstrasse, Geb. 30.45, 76128 Karlsruhe, Germany

$$CuBr_2 + 3Fe(OOCCH_3)_2 + [nPr_3N(CH_2)_6NnPr_3]Br_2 \xrightarrow[CH_3CN/Et_2O]{+\ 6\ PhSeSiMe_3} (nPr_3N(CH_2)_6NnPr_3)[CuFe_3Br_3(SePh)_6]\ (\mathbf{1})$$

Scheme 1.

$$CuOOCCH_3 + 0.2\ FeCl_2 + 1.5\ PPh_3 \xrightarrow[DME]{+\ 1.6\ PhSeSiMe_3} [Cu_5Fe(SePh)_7(PPh_3)_4]\ (\mathbf{2})$$

Scheme 2.

$$CuOOCCH_3 + 0.8\ FeCl_2 + 4\ PPh_3 \xrightarrow[dme]{+\ 3\ PhSeSiMe_3} [Cu_4Fe_3(SePh)_{10}(PPh_3)_4]\ (\mathbf{3})$$

Scheme 3.

Crystal Structures

Ionic **1** crystallizes in the trigonal space group $P\bar{3}$ with three crystallographically independent $[CuFe_3Br_3(SePh)_6]^{2-}$ cluster anions, two of which reside on a threefold and one on a $\bar{3}$ axis (see Experimental Section for further details). Because the structures of the cluster cores, including bond lengths and angles, are quite similar for all three, only one of them is discussed in the following. The cluster anion $[CuFe_3Br_3(SePh)_6]^{2-}$ (Figure 1) consists of a six-membered $Fe_3(SePh)_3$ ring in a chair conformation that is capped by a nearly trigonal-planar $Cu(SePh)_3$ unit [Cu, Se(1), Se(1′), Se(1′′); Se–Cu–Se = 119.96(1)°]. A threefold axis runs through the copper atom and the center of the hexanuclear ring, and the copper atom is slightly shifted by 4.7 pm from the triangular selenium face towards the iron atoms (mean Cu–Fe distance of 339.2 pm). Each of the iron atoms is additionally coordinated by a terminal bromido ligand to give a distorted tetrahedral coordination environment for the iron atoms [Fe–Br = 241.7(2) pm]. The metal–selenium distances are found to be longer for iron [246.7–246.8(2) pm] than for copper [234.2–234.3(1) pm], which is most probably a result of the different coordination modes. This adamantoid cluster core in **1** is therefore similar to the structures of $[CuFe_3Cl_3(EiPr)_6]^{2-}$ (E = Se, S), which have been crystallized previously with singly charged ammonium cations.[16,17]

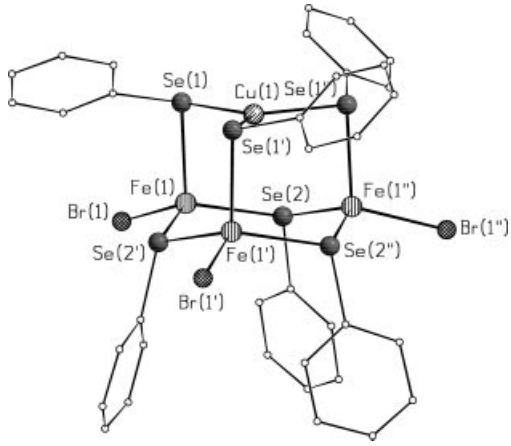

Figure 1. Molecular structure of the cluster anion $[CuFe_3Br_3(SePh)_6]^{2-}$ in $[nPr_3N(CH_2)_6NnPr_3][CuFe_3Br_3(SePh)_6]$ (**1**). C and H atoms omitted for clarity. Selected bond lengths [pm] and angles [°]: Se(1)–Cu(1) 234.2(1), Se(1)–Fe(1) 247.3(2), Se(2)–Fe(1) 246.7(2), Se(2)–Fe(1′) 246.8(2), Cu(1)–Se(1′′) 234.3(1), Cu(1)–Se(1′) 234.3(9), Br(1)–Fe(1) 241.7(2), Fe(1)–Se(2′′) 246.8(2); Fe(1)–Se(2)–Fe(1′) 112.64(6), Se(1)–Cu(1)–Se(1′′) 119.96(1), Se(1)–Cu(1)–Se(1′) 119.96(1), Se(1′′)–Cu(1)–Se(1′) 119.96(1), Br(1)–Fe(1)–Se(2) 109.71(6), Br(1)–Fe(1)–Se(2′′) 115.11(6), Se(2)–Fe(1)–Se(2′′) 118.86(6), Br(1)–Fe(1)–Se(1) 108.00(6), Se(2)–Fe(1)–Se(1) 103.55(6), Se(2′′)–Fe(1)–Se(1) 99.87(6). Symmetry transformations for the generation of equivalent atoms: ′: $1 - y, x - y, z$; ′′: $-x + y + 1, -x + 1, z$.

Cluster **2** crystallizes in the monoclinic space group $P2_1/c$ (Figure 2). The structure comprises a central Cu_3Fe trigonal pyramid formed by Cu(1), Cu(2), Cu(3), and Fe(1) [Cu···Cu = 430.1–451.4(1); Cu···Fe = 403.0–417.2(1) pm] with the six edges bridged by $SePh^-$ ligands [Se(1)–Se(6); Cu–Se = 244.4–270.9(1); Fe(1)–Se = 242.9–249.5(1) pm]. One additional copper atom [Cu(4)] is bonded to this adamantoid cluster cage through the three selenium atoms of the basal six-membered ring [Se(1)–Se(3); Cu–Se = 242.0–249.0(1) pm], which displays only a weak chair conformation [maximum deviation of 66.5 pm for Se(3) from the trigonal plane formed by Cu(1)–Cu(3)]. The coordination environment of Cu(4) is trigonal-planar [sum of Se–Cu(4)–Se angles is 360°]. The copper atoms Cu(1)–Cu(3) which form the basal plane of the Cu_3Fe pyramid are each additionally coordinated by a terminal PPh_3 ligand to result in an overall distorted tetrahedral coordination environment for these atoms. Fe(1), at the apex of the Cu_3Fe pyramid, is additionally coordinated by another $SePh^-$ ligand [Se(7)], and a further $CuPPh_3$ unit is attached through this and two other $SePh^-$ ligands [Se(5), Se(6), Se(7)] to the adamantoid cluster cage.

Compound **3** crystallizes in the monoclinic space group $P2_1/c$ (Figure 3). Similar to **1**, the structure contains a central $CuFe_3$ trigonal pyramid formed by Fe(1), Fe(2), Fe(3), and Cu(4) [Fe···Cu = 393.1–420.5(2); Fe···Fe = 402.1–410.2 pm]. Thus, three iron atoms define the vertices of the basal triangular plane, which is bridged by a μ_3-$SePh^-$ ligand [Fe–Se(10) = 250.1–251.2(2) pm], while the apex of the pyramid is occupied by a $CuPPh_3$ unit [Cu(4)–P(4) =

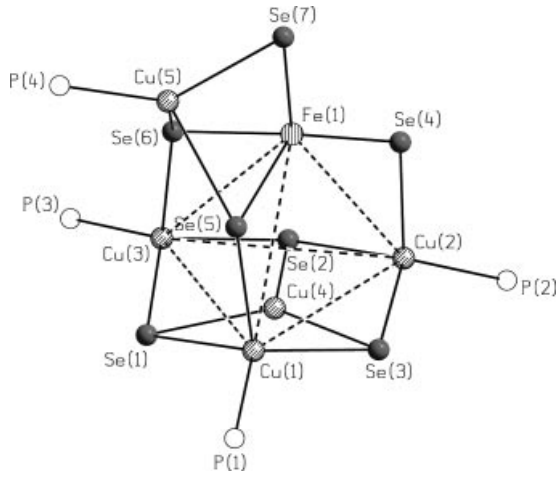

Figure 2. Molecular structure of $[Cu_5Fe(SePh)_7(PPh_3)_4]$ (**2**). C and H atoms omitted for clarity. Selected bond lengths [pm]: Fe(1)–Se(4) 2.4294(12), Fe(1)–Se(7) 247.7(1), Fe(1)–Se(5) 248.9(1), Fe(1)–Se(6) 249.5(1), Se(1)–Cu(4) 249.0(1), Se(1)–Cu(3) 249.5(1), Se(1)–Cu(1) 256.3(1), Se(2)–Cu(4) 243.7(1), Se(2)–Cu(2) 249.5(1), Se(2)–Cu(3) 254.1(1), Se(3)–Cu(4) 242.0(1), Se(3)–Cu(1) 252.1(1), Se(3)–Cu(2) 270.8(1), Se(4)–Cu(2) 244.4(1), Se(5)–Cu(1) 247.8(1), Se(5)–Cu(5) 261.5(1), Se(6)–Cu(3) 254.3(1), Se(6)–Cu(5) 258.0(1), Se(7)–Cu(5) 244.4(1), Cu(1)–P(1) 223.7(2), Cu(2)–P(2) 226.4(2), Cu(3)–P(3) 225.4(2), Cu(5)–P(4) 221.1(2); nonbonding metal–metal distances: Cu(1)–Cu(4) 254.6(1), Cu(2)–Cu(4) 263.6(1), Cu(3)–Cu(4) 261.4(1), Cu(5)–Fe(1) 266.2(1) (not drawn), Cu(1)–Cu(2) 451.4, Cu(1)–Cu(3) 430.1, Cu(2)–Cu(3) 442.0, Cu(1)–Fe(1) 403.7, Cu(2)–Fe(1) 403.0, Fe(1)–Cu(3) 417.2 (dashed lines).

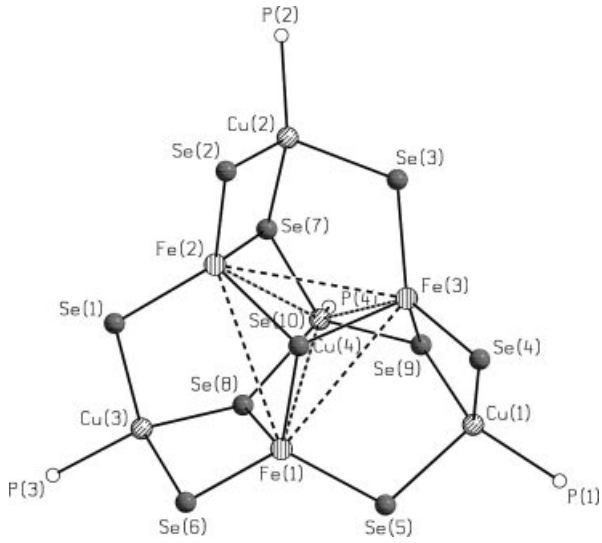

Figure 3. Molecular structure of $[Cu_4Fe_3(SePh)_{10}(PPh_3)_4]$ (**3**). C and H atoms omitted for clarity. Selected bond lengths [pm]: Se(7)–Fe(2) 249.4(2), Se(7)–Cu(4), 251.6(2) Se(7)–Cu(2) 252.1(2), Se(8)–Cu(4) 246.9(2), Se(8)–Fe(1) 247.3(2), Se(8)–Cu(3) 250.6(2), Se(9)–Cu(4) 246.9(2), Se(9)–Fe(3) 247.4(2), Se(9)–Cu(1) 256.9(2), Se(10)–Fe(2) 250.1(2), Se(10)–Fe(1) 250.9(2), Se(10)–Fe(3) 251.2(2), Se(1)–Fe(2) 244.8(2), Se(1)–Cu(3) 247.5(2), Se(2)–Fe(2) 245.5(2), Se(2)–Cu(2) 248.7(2), Se(3)–Fe(3) 246.6(2), Se(3)–Cu(2) 250.6(2), Se(4)–Fe(3) 244.1(2), Se(4)–Cu(1) 247.4(2), Se(5)–Fe(1) 244.0(2), Se(5)–Cu(1) 245.6(2), Se(6)–Fe(1) 243.1(2), Se(6)–Cu(3) 250.3(2), Cu(1)–P(1) 226.1(3), Cu(2)–P(2) 224.7(3), Cu(3)–P(3) 226.1(3), Cu(4)–P(4) 223.7(3); shortest nonbonding metal–metal distances: Cu(1)–Fe(3) 301.6(2), Cu(2)–Fe(2) 306.4(2), Cu(3)–Fe(1) 304.5(2) (not drawn), Cu(4)–Fe(1) 397.1(2), Cu(4)–Fe(2) 420.5(2), Cu(4)–Fe(3) 393.0(2), Fe(1)–Fe(2) 409.7(2), Fe(1)–Fe(3) 410.2(2), Fe(2)–Fe(3) 402.0(2) (dashed lines).

223.7(3) pm]. The other faces of the pyramid are capped by three distorted tetrahedral $PPh_3Cu(SePh)_3$ units in such a way that six $SePh^-$ ligands [Se(1)–Se(6)] adopt a μ_2- and three [Se(8)–Se(9)] a μ_3-bridging mode, which results in an overall distorted tetrahedral coordination of the metal atoms. All copper atoms are surrounded by two μ_2-$SePh^-$ moieties [mean Cu–Se distance of 248.4(2) pm], one μ_3-$SePh^-$ [mean Cu–Se distance of 250.8(2) pm], and a terminal PPh_3 ligand [mean Cu–P distance of 252.2(3) pm]. The iron atoms are four-coordinated by two μ_2-$SePh^-$ [mean Fe–Se distance of 244.7(2) pm] and two μ_3-$SePh^-$ ligands [mean Fe–Se distance of 249.5(2) pm]. Obviously, the core of the cluster complex comprises a pseudo-threefold axis running through Se(10), Cu(4), and P(4); however, the organic ligands do not have this symmetry.

Optical Spectra

The UV/Vis spectra of **1**–**3** measured as a mull in nujol between quartz plates display several absorption features in the region between 600 and 220 nm. The spectrum of **1** displays a very broad shoulder around 370 nm, another one at 275 nm, and a peak at 249 nm. The spectrum of **2** consists of two shoulders around 450 and 290 nm, while that of **3** shows a broad absorption maximum at 440 nm followed by a shoulder at 280 nm (Figure 4). In solution (**1** in CH_3CN; **2**, **3** in thf), the ratio of the maxima and shoulders at higher wavelengths to those below 350 nm increases compared to the spectra measured in nujol. Compounds **1** and **3** display a shoulder at 390 (ε = 7409) and 415 nm (ε = 6868), respectively, while the corresponding feature of **2** is most probably obscured by the tail of the following intense band with a maximum at 272 nm ($\varepsilon = 8.87 \times 10^4$ $M^{-1}cm^{-1}$). This band is followed by a very weak shoulder at 252 nm ($\varepsilon = 8.756 \times 10^4$ $M^{-1}cm^{-1}$). Two similar features are observed for **3** at 270 ($\varepsilon = 1.092 \times 10^5$) and 255 nm ($\varepsilon = 1.142 \times 10^5$ $M^{-1}cm^{-1}$), while **1** displays only one broad additional absorption maximum at 250 nm ($\varepsilon = 6.802 \times 10^4$ $M^{-1}cm^{-1}$). A detailed assignment of the bands is complicated as there are several possible absorption processes for the compounds. However, due to their relatively low extinction coefficients of about 7000 $M^{-1}cm^{-1}$, it is possible that the broad bands at higher wavelengths originate from spin-allowed d–d transitions in tetrahedrally coordinated Fe^{2+} while the intense bands at lower wavelengths correspond to either Se→Cu or Se→Fe charge-transfer bands partially overlapped by π–π* transitions of the $SePh^-$ and/or PPh_3 ligands.

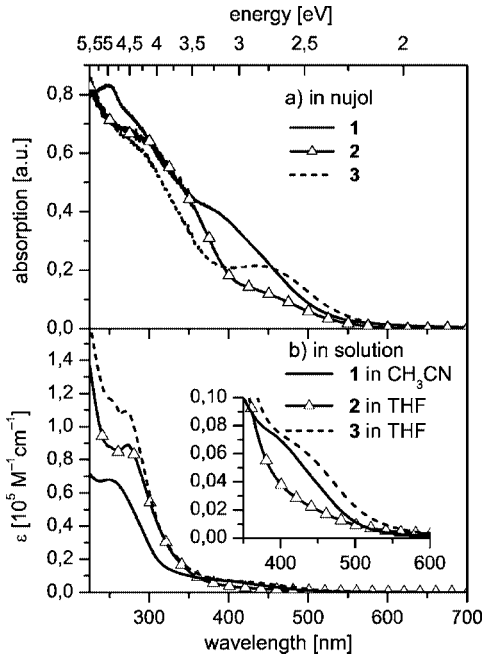

Figure 4. UV/Vis spectra of $(n\text{Pr}_3\text{N}(\text{CH}_2)_6\text{N}n\text{Pr}_3)[\text{CuFe}_3\text{Br}_3(\text{SePh})_6]$ (**1**), $[\text{Cu}_5\text{Fe}(\text{SePh})_7(\text{PPh}_3)_4]$ (**2**), and $[\text{Cu}_4\text{Fe}_3(\text{SePh})_{10}(\text{PPh}_3)_4]$ (**3**) as mulls in nujol (a) and in solution (b).

Thermogravimetric Analysis

The decomposition of **2** and **3** upon heating was monitored by TGA in vacuo (Figure 5). The mass changes of **2** and **3** both display one-step processes due to the cleavage of most of the ligands, although the temperature range of the cleavage is much narrower for **3** (125–275 °C) than for **2** (125–375 °C). The observed mass losses of 76.2% (**2**) and 75.1% (**3**) agree with the calculated values [loss of 3.5 SePh_2 and four PPh_3 molecules for **2** (76%) and five SePh_2 and four PPh_3 molecules for **3** (73.7%)]. The powder diffraction patterns (Figure 6) of the residues indicate the formation of mixtures of the known phases Cu_2Se[18] and CuFeSe_2.[19] The thermal treatment of **2** should result in a powder with the theoretical composition $\text{Cu}_5\text{FeSe}_{3.5}$. The ratio of the peak intensities of the different patterns reveals a higher amount of Cu_2Se in comparison to CuFeSe_2, although two peaks at 2θ = 44.8° and 47.9°, which have been marked with an asterisk, could not be assigned. For **3**, the residue should have the composition $\text{Cu}_4\text{Fe}_3\text{Se}_5$, which is much closer to the formula of the ternary solid-state phase CuFeSe_2 than that of the residue of **2**. In agreement with this, the powder pattern corresponds to a larger fraction of CuFeSe_2 and a smaller fraction of Cu_2Se.

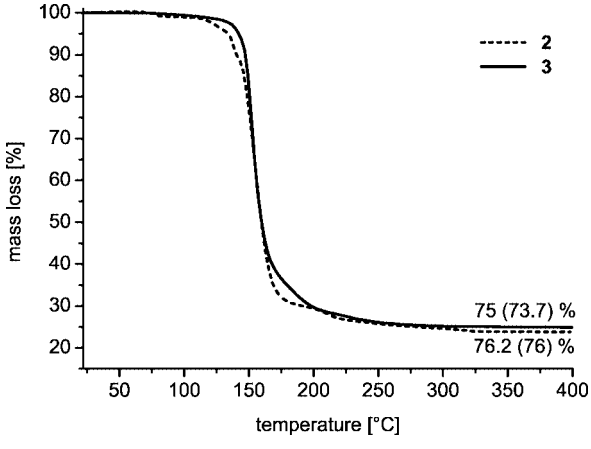

Figure 5. Thermogravimetric analysis of $[\text{Cu}_5\text{Fe}(\text{SePh})_7(\text{PPh}_3)_4]$ (**2**) and $[\text{Cu}_4\text{Fe}_3(\text{SePh})_{10}(\text{PPh}_3)_4]$ (**3**) in vacuo. Theoretical values for the calculated mass loss of 4 PPh_3/3.5 SePh_2 in **2** and 4 PPh_3/5 SePh_2 in **3** are given in parentheses.

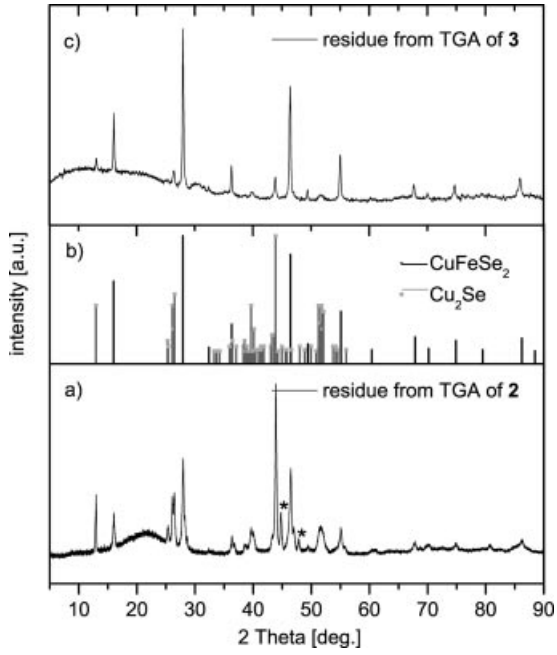

Figure 6. Powder diffraction patterns of a) the residue of the TGA of $[\text{Cu}_5\text{Fe}(\text{SePh})_7(\text{PPh}_3)_4]$ (**2**). Peaks marked by an asterisk cannot be assigned; b) monoclinic α-Cu_2Se (grey lines)[18] and tetragonal CuFeSe_2 (black lines);[19] c) residue of the TGA of $[\text{Cu}_4\text{Fe}_3(\text{SePh})_{10}(\text{PPh}_3)_4]$ (**3**).

Conclusion

The raction of mixtures of copper and iron salts with PhSeSiMe_3 can be used for the synthesis of mixed-metal Cu/Fe/Se cluster molecules. Different structures are formed depending on the kind of ligands and the ratio of the precursor compounds. Thermal cleavage of the organic ligands results in the formation of mixtures of binary Cu_2Se and ternary CuFeSe_2, the ratio of which depends on the ratio of the elements in the precursor cluster molecules.

Experimental Section

Synthesis: Standard Schlenk techniques were employed throughout the syntheses using a double-manifold vacuum line (10^{-3} mbar) with high-purity nitrogen (99.9999%). Diethyl ether, and dme were dried with sodium/benzophenone, CH_3CN with CaH_2, and all were distilled under nitrogen. CuCl was washed with HCl, CH_3OH, and diethyl ether to remove traces of CuCl_2, and then dried under vac-

uum. $CuOOCCH_3$[20] and $PhSeSiMe_3$[21] were prepared according to literature procedures.

Physical Measurements: UV/Vis absorption spectra of cluster molecules in solution were measured with a Varian Cary 500 spectrophotometer in quartz cuvettes. Solid-state UV/Vis spectra were measured as a mull in nujol between quartz plates with a Labsphere integrating sphere. Thermogravimetric analyses were run with a thermobalance STA 409 from Netzsch in vacuo (heating rate 2 K min^{-1}).

[*n*Pr$_3$N(CH$_2$)$_6$N*n*Pr$_3$]Br$_2$: 1,6-Diaminohexane (8.3 mL, 0.07 mol), *n*-propyl bromide (39.4 mL, 0.43 mol) and $NaHCO_3$ (28 g, 0.33 mol) were added to 120 mL of a 1:1 mixture of H_2O and CH_3CN. Two liquid phases and one solid phase were formed. The mixture was then heated under reflux and the formation of CO_2 indicated the reaction progress. After 2 d, once the solid phase had disappeared, the organic phase was separated and the solvent evaporated to dryness. The residue was then treated with 100 mL of $CHCl_3$ to precipitate NaBr. Removal of this solid by filtration and renewed evaporation of the solvent yielded [*n*Pr$_3$N(CH$_2$)$_6$N*n*Pr$_3$]Br$_2$ as a pale-yellow precipitate. Yield: 8.56 g (23%). $C_{24}H_{54}Br_2N_2$ (531.61): calcd. C 54.38, H 10.26, N 5.28, found C 53.13, H 10.82, N 5.06.

[*n*Pr$_3$N(CH$_2$)$_6$N*n*Pr$_3$][CuFe$_3$Br$_3$(SePh)$_6$] (1): CuBr (50 mg, 0.35 mmol), Fe(OOCCH$_3$)$_2$ (183 mg, 1.05 mmol), and [*n*Pr$_3$N(CH$_2$)$_6$N*n*Pr$_3$]Br$_2$ (185 mg, 0.35 mmol) were suspended in 40 mL of CH_3CN. After 1 d of stirring, $PhSeSiMe_3$ (0.44 mL, 2.1 mmol) was added at 0 °C and the mixture warmed to room temperature which led to the formation of red-orange crystals of **1**. Yield: 530 mg (73%). $C_{60}H_{84}Br_3CuFe_3N_2Se_6$ (1644.6): calcd. C 40.5, H 4.8, N 1.6; found C 40.9, H 4.9, N 1.8.

[Cu$_5$Fe(SePh)$_7$(PPh$_3$)$_4$] (2): $CuOOCCH_3$ (100 mg, 0.82 mmol), $FeCl_2$ (21 mg, 0.16 mmol), and PPh_3 (0.32 g, 1.2 mmol) were suspended in 30 mL of dme. After 1 d of stirring, $PhSeSiMe_3$ (0.32 mL, 1.39 mmol) was added at –30 °C and the mixture warmed to room temperature to give a clear red solution. After 1 d, the reaction solution was layered with 50 mL of pentane by autothermal condensation. Red, needle-like crystals of **2** grew over several days. Yield: 308 mg (75%). $C_{114}H_{95}Cu_5FeP_4Se_7$ (2515.1): calcd. C 54.4, H 3.81; found C 54.5, H 4.10.

[Cu$_4$Fe$_3$(SePh)$_{10}$(PPh$_3$)$_4$] (3): $CuOOCCH_3$ (100 mg, 0.82 mmol), $FeCl_2$ (86 mg, 0.68 mmol), and PPh_3 (0.86 g, 3.3 mmol) were suspended in 100 mL of dme. After 1 d of stirring, $PhSeSiMe_3$ (0.57 mL, 2.46 mmol) was added to give a red solution. After another day, approximately 1/3 of the solvent was removed by condensation, which resulted in the immediate crystallization of orange, plate-like needles of **3**. Yield: 460 mg (74%). $C_{132}H_{110}Cu_4Fe_3P_4Se_{10}$ (3031.5): calcd. C 52.3, H 3.7; found C 52.6, H 4.0.

Crystallography: Crystals suitable for single-crystal X-ray diffraction were taken directly from the reaction solution of the compound and then selected in perfluoroalkyl ether oil. Single-crystal X-ray diffraction data of **1** and **2** were collected using graphite-monochromatized Mo-K_α radiation (λ = 0.71073 Å) with a STOE IPDS II (Imaging Plate Diffraction System) equipped with a Schneider rotating anode. Single-crystal X-ray diffraction data of **3** were collected using synchrotron radiation (λ = 0.80 Å) with a STOE IPDS II (Imaging Plate Diffraction System) at the ANKA synchrotron source in Karlsruhe. Further details are given in Table 1. The structures were solved with the direct-methods program SHELXS[22] of the SHELXTL PC program suite, and were refined with the use of the full-matrix least-squares program SHELXL.[22] Molecular diagrams were prepared using SCHAKAL 97.[23] All Cu, Fe, Se, Br, P, Cl, and C atoms of the cluster molecules were refined with anisotropic displacement parameters with the exception of **3**, whose C atoms were refined isotropically. In addition, split positions with isotropic displacement parameters were calculated in **1** for the C atoms of the phenyl rings C11, C12, C20, C21, and C22 as well as of the *n*-propyl groups of the ammonium salt C43, C44, C45, and C57. N and C atoms of the solvent molecules were refined isotropically. H atoms were calculated in fixed positions for **2** and **3**. CCDC-612653 (**1**), -612654 (**2**) and -612655 (**3**) contain the supplementary crystallographic data for this paper. These data can be obtained free of charge from The Cambridge Crystallographic Data Center via www.ccdc.cam.ac.uk/data_request/cif. X-ray powder diffraction patterns were recorded with a STOE STADI P diffractometer (Cu-$K_{\alpha1}$ radiation, germanium monochromator, Debye–Scherrer geometry) in sealed glass capillaries.

Table 1. Crystallographic data for [*n*Pr$_3$N(CH$_2$)$_6$N*n*Pr$_3$][CuFe$_3$Br$_3$(SePh)$_6$] (**1**), [Cu$_5$Fe(SePh)$_7$(PPh$_3$)$_4$] (**2**), and [Cu$_4$Fe$_3$(SePh)$_{10}$(PPh$_3$)$_4$] (**3**).

	1·0.5CH$_3$CN	**2**	**3**·dme
Formula mass [g mol^{-1}]	1798.4	2515.1	3121.5
Crystal system	trigonal	monoclinic	monoclinic
Space group	$P\bar{3}$	$P2_1/n$	$P2_1/c$
a [pm]	2315.1(3)	1471.2(3)	1660.5(3)
b [pm]	2315.1(3)	2768.4(6)	5227.9(11)
c [pm]	2304.6(5)	2663.5(5)	1540.6(3)
β [°]		92.60(3)	113.44(3)
V [10^9 pm^3]	10697(3)	10837(4)	12270(4)
Z	6	4	4
T [K]	190	180	150
D_c [g cm^{-3}]	1.675	1.541	1.690
$\mu(\lambda)$ [mm^{-1}]	5.671 (Mo-K_α)	3.550 (Mo-K_α)	5.552 (0.80 Å)
F(000)	5310	4992	6184
$2\theta_{max}$ [°]	50	50	46
Measd. reflns.	33328	46983	25256
Unique reflns.	11964	18081	9924
R_{int}	0.0556	0.0421	0.1056
Reflns. with $I > 2\sigma(I)$	7086	14080	8261
Refined parameters	680	1180	754
R_1 [$I > 2\sigma(I)$][a]	0.0592	0.0519	0.0480
wR_2 (all data)[b]	0.1771	0.1547	0.1465

[a] $R_1 = \Sigma||F_o| - |F_c||/\Sigma|F_o|$. [b] $wR_2 = \{\Sigma[w(F_o^2 - F_c^2)^2]/\Sigma[w(F_o^2)^2]\}^{1/2}$.

Acknowledgments

This work was supported by the Deutsch–Israelisches Programm (DIP) and the Deutsche Forschungsgemeinschaft (Center for Functional Nanostructures CFN). The authors are grateful to Dr. S. Chitsaz for performing the TGA experiments.

[1] W. Hirpo, S. Dhingra, M. Kanatzidis, *J. Chem. Soc., Chem. Commun.* **1992**, 557–559.
[2] J. Olkowska-Oetzel, D. Fenske, P. Scheer, A. Eichhöfer, *Z. Anorg. Allg. Chem.* **2003**, *629*, 415–420.
[3] A. Eichhöfer, D. Fenske, *J. Chem. Soc., Dalton Trans.* **2000**, 941–944.
[4] R. Ahlrichs, A. Eichhöfer, D. Fenske, O. Hampe, M. M. Kappes, P. Nava, J. Olkowska-Oetzel, *Angew. Chem.* **2004**, *116*, 3911–3915; *Angew. Chem. Int. Ed.* **2004**, *43*, 3823–3827.
[5] D. T. T. Tran, L. M. C. Beltran, C. M. Kowalchuk, N. R. Trefiak, N. J. Taylor, J. F. Corrigan, *Inorg. Chem.* **2002**, *41*, 5693–5698.

[6] D. T. T. Tran, N. J. Taylor, J. F. Corrigan, *Angew. Chem.* **2000**, *112*, 965–967; *Angew. Chem. Int. Ed.* **2000**, *39*, 935–937.
[7] A. Lorenz, D. Fenske, *Angew. Chem.* **2001**, *113*, 4537–4541; *Angew. Chem. Int. Ed.* **2001**, *40*, 4402; A. Lorenz, D. Fenske, *Z. Anorg. Allg. Chem.* **2001**, *627*, 2232–2248.
[8] R. Pätow, D. Fenske, *Z. Anorg. Allg. Chem.* **2002**, *628*, 1279–1288.
[9] M. W. DeGroot, N. J. Taylor, J. F. Corrigan, *J. Am. Chem. Soc.* **2003**, *125*, 864–865.
[10] A. Kornienko, S. Banerjee, G. A. Kumar, R. E. Riman, T. J. Emge, J. G. Brennan, *J. Am. Chem. Soc.* **2005**, *127*, 14008–14014.
[11] W. Hirpo, S. Dhingra, A. C. Sutorik, M. Kanatzidis, *J. Am. Chem. Soc.* **1993**, *115*, 1597–1599.
[12] V. Soloviev, A. Eichhöfer, D. Fenske, U. Banin, *J. Am. Chem. Soc.* **2000**, *122*, 2673–2674.
[13] V. Soloviev, A. Eichhöfer, D. Fenske, U. Banin, *J. Am. Chem. Soc.* **2001**, *123*, 2354–2364.
[14] J. Lazewski, H. Neumann, H. Parlinski, *Phys. Rev. B* **2004**, *70*, 195206.
[15] N. Hamdadou, M. Morsli, A. Khelil, J. C. Bernède, *J. Phys. D: Appl. Phys.* **2006**, *39*, 1042–1049.
[16] H.-O. Stephan, G. Henkel, M. G. Kanatzidis, *Chem. Commun.* **1997**, 67–68.
[17] J. Lackmann, R. Hauptmann, S. Weißgräber, G. Henkel, *Chem. Commun.* **1999**, 1995–1996.
[18] In Powder Diffraction File PDF-2 Database Sets 1–85, **1993**, International Center for Diffraction Data, Newtown Square USA, file number 27-1131; A. L. N. Stevels, *Philips Res. Rep. Suppl.* **1969**, *9*, 39–44.
[19] In Powder Diffraction File PDF-2 Database Sets 1–85, **1993**, International Center for Diffraction Data, Newtown Square USA, file number 44-1305; J. Henao, J. Delgado, M. Quintero, *Powder Diff.* **1994**, *9*, 108.
[20] D. A. Edwards, R. Richards, *J. Chem. Soc., Dalton Trans.* **1973**, 2463–2468.
[21] N. Miyoshi, H. Ishii, K. Kondo, S. Mui, N. Sonoda, *Synthesis* **1979**, 301–304.
[22] G. M. Sheldrick, *SHELXTL, An Integrated System for Solving, Refining, and Displaying Crystal Structures from Diffraction Data*, PC version 5.1, Bruker Analytical X-ray Systems, Karlsruhe, **2000**.
[23] E. Keller, *SCHAKAL 97, A Computer Program for the Graphic Representation of Molecular and Crystallographic Models*, University of Freiburg, **1997**.

Received: July 4, 2006
Published Online: November 17, 2006

